Economic and Optimal Dispatch Model of Electricity, Heat and Gas for Virtual Power Plants in Parks Considering Low Carbon Targets

Wei-Guo Zhang, Qing Zhu, Hong-Juan Zheng, Lin-Lin Gu and Hui-Jie Lin

Abstract—**To promote the consumption and development of new and green energy sources, we propose an economically optimal dispatch model to simulate virtual power plants (VPPs) in parks considering low-carbon objectives based on a dual-carbon background. First, individual models involved in the optimal dispatch of VPPs are introduced. A two-stage operation process of electricity-to-hydrogen transformation and hydrogen methanation of power-to-gas equipment is refined and analysed. Unstable wind power is converted into hydrogen and supplied to the hydrogen load during the electrolysis of the water-to-hydrogen stage in conjunction with the development of hydrogen energy demands. Second, to minimise the sum of operating and carbon emission costs, an optimal dispatch model utilised by the virtual power plant considering a low-carbon objective is established. A simulation of the calculation case shows that the proposed model can achieve efficient energy utilisation and improved economic and carbon costs for a VPP in the park. Finally, a sensitivity analysis of the system cost is conducted by adding weighting coefficients; the optimal range of weighting coefficients for the VPP in the park proposed in this paper are derived for reference by considering economic benefits and environmental protection.**

Index Terms—**carbon emissions, virtual power plant, power-to-gas, demand response, optimal dispatch**

I. Introduction

In recent years, as energy, climate and environmental challenges have worsened, countries have been making changes to their energy structures, and energy consumption has gradually shifted to various renewable energy sources. It is estimated that China's annual carbon emissions are approximately 10 billion tonnes, China has a great responsibility to reduce carbon emissions as it is world's largest carbon emitter[1]. To slow the depletion of fossil fuel sources and reduce pollution in the environment, the integrated energy supply of electricity, heat and gas has flourished by achieving a complementary combined supply between multiple energy sources and improving the efficiency of primary energy use [2-5]. Among these sources, virtual power plants (VPPs) have focused on the coupling of multiple energy flows, which allows the mutual transformation and transmission of electricity, heating, cooling and gaseous forms of energy. VPPs also allow for the overall planning and operational coordination and optimisation of the distribution, transformation, storage and consumption of multiple energy sources to realise diversified energy supplies, energy services and energy use methods.

VPPs achieve internal collaborative optimisation by aggregating multiregional, large-scale distributed energy sources and participating in overall grid dispatch [5-6]. A multiobjective optimal VPP scheduling model, including distributed power supply, electric vehicles, and loads, was constructed in [7], and an interruptible load (IL) in the form of a demand response was considered in the electric load. Some researchers [8] have studied the optimal coordinated VPP scheduling in the main electricity market and rotating standby market. This VPP aggregated distributed power sources and electrical loads. Other researchers [9] have proposed a coordinated optimal dispatch model of electric and thermal VPPs with microgas turbines (MTs), gas boilers and energy storage devices. Additionally, some scholars [10] have studied VPPs from the perspective of demand response and have established an incentive- and price-based demand response VPP model. Other scholars [11] have aggregated a multiregion VPP integrated energy optimisation dispatch model for cogeneration units, gas boilers and wind turbines. Researchers [12] have also established a VPP optimal dispatch model including MTs, gas boilers, distributed power sources, and electric vehicles. Existing studies have mainly focused on external participation in the main electricity market; they rarely involve VPP participation in the heat market or the gas market and only realise the optimal dispatch of electricity [7-10] or the coordinated optimal dispatch between electricity and heat [11-12] for VPPs, failing to realise the coordinated optimal dispatch among multiple energy sources.

More and more people pay attention to the optimal dispatch

Manuscript received June 25, 2022; revised November 25, 2022.

This work is supported by Science and Technology project of State Grid Corporation（Research and application of zero-carbon evolution technology of micro energy grids in national carbon neutral parks, NO. 5100-202118566A-0-5-SF）.

Wei-guo Zhang is a PhD candidate at Southeast University, Nanjing 210096, China (Corresponding author: e-mail: 230209330@seu.edu.cn)

Qing Zhu is a senior engineer of NARI-TECH Nanjing Control Systems Co., Ltd., Nanjing 211106, China (e-mail: zhuqing1@sgepri.sgcc.com.cn)

Hong-juan Zheng is a mid-level engineer of NARI-TECH Nanjing Control Systems Co., Ltd., Nanjing 211106, China (e-mail: zhenghongjuan@sgepri.sgcc.com.cn)

Lin-lin Gu is a mid-level engineer of NARI-TECH Nanjing Control Systems Co., Ltd., Nanjing 211106, China (e-mail: gulinlin@sgepri.sgcc.com.cn)

Hui-jie Lin is a mid-level engineer of NARI-TECH Nanjing Control Systems Co., Ltd., Nanjing 211106, China (e-mail: linhuijie@sgepri.sgcc.com.cn)

problem of VPPs. The objectives adopted in the economic dispatch model include the minimum total cost and the maximum total profit [13]-[15]. In reference [16], a VPP–load game model was developed with the highest VPP return as the objective function. In reference [17], researchers developed an economically optimised dispatch model for a VPP by adding electric vehicles to enhance its flexibility. In [18], VPPs in separate regions were optimised with the objective of maximising their overall revenue, and bidding strategies for VPP participation in the different markets were obtained. In reference [19], researchers have proposed a VPP scheduling approach with two stages in order to study impact of energy storage equipment and customer revenue on VPP revenue. Some scholars [20] considered the uncertainties of electricity prices over time and developed an improved VPP multistage stochastic optimisation model. In reference [21], in order to obtain the best operational strategy to promote new energy consumption, the researchers established a two-level electricity-thermal energy trading strategy with an objective function to reduce the cost of energy acquired by the VPP.

The above studies have mainly enhanced the operational performance of the energy market by adding energy storage devices, improving the dispatching strategy and tapping into the demand response of consumers; this strategy lacks the complexity of energy migration, and it assumes the minimisation of operational costs as the objective optimisation function without sufficiently considering carbon emission costs.

According to data published by the International Energy Agency, carbon emissions from industrial parks in China account for approximately 31% of the country's total emissions and exhibit continuous growth. As the core unit of industrial clustering and development, industrial parks have become a driving force in China's economic growth and an important factor for achieving scientific and precise carbon emission reduction and eventual carbon neutrality [22-24]. Based on the above analysis, we take a park as the context for our study, consider the operating and carbon emission costs of a VPP in the park, and assemble a two-stage power-to-gas conversion model with the minimal costs for all systems in the park as the scheduling target. Through this study, we refine power-to-gas (P2G) conversion into a two-stage operation of electricity-to-hydrogen transformation and hydrogen methanation, prioritising the high-grade utilisation of hydrogen energy in the hydrogen production link, which can reduce the energy loss caused by step conversion in the whole operation process. The energy loss caused by conversion can be reduced throughout the operation process. A VPP that aggregates multiple energy sources is constructed, and an optimal control model under multiple scenarios is determined by using CPLEX with YALMIP in MATLAB to evaluate the recommended model's performance.

II. System structure of the VPP

The VPP system covers a wide range of energy supply and conversion devices, including wind power plants (WPPs), PV generators, combined heat and power (CHP), P2G, gas boilers and energy storage devices. The system can prioritise the advantages of interactively coupling electricity, heat and gas to achieve synergistic optimisation among different energy sources vertically, coordinate and optimise each type of energy in the production, transmission and distribution horizontally, while the user-side interaction is fully tapped, which effectively improves the flexibility of the the source network, and is connected to the information interaction systems of the electricity, heat and gas networks to take part in the large grid dispatch model, reduce carbon costs and optimise system profits [24]. In this paper, a VPP system in the park which contains P2G is constructed, as shown below.

The supply side is supplied by distributed energy, the upper grid and the gas grid, which provide the energy source for the system; The conversion side contains the electrolysis tank, hydrogen storage tank and methane reactor unit for P2G system, the waste heat boiler and gas turbine unit for CHP units and the gas boiler unit; The combined electrical, gas, hydrogen and thermal loads form the load side of the system.

The electrolysis tank converts potentially discarded wind-generated or low-cost electricity into hydrogen, part of which is injected into the natural gas (NG) system via a methane reactor to produce methane for direct supply to the gas load or gas turbine cogeneration, reducing the amount of gas purchased from the upper gas grid and reducing the system's energy purchase costs. The remaining portion, which can achieve the arbitrage of "high generation and low storage," is stored in the hydrogen storage tanks and supplied towards the hydrogen load during the times when electricity prices are at their highest. This reduces the energy loss brought on by the methanation step's use and increases the system's overall efficiency in terms of energy utilization.

China's first power-to-gas conversion unit using wind and solar energy has been completed in Dalian and has achieved good results. In the future, as the relevant technology develops and matures, the use of the above-mentioned multi-energy coupled units to optimise VPP scheduling and operation will achieve even better economic benefits. Therefore, this paper studies the optimal scheduling of VPP with power to gas conversion, which is forward-looking and of theoretical guidance.

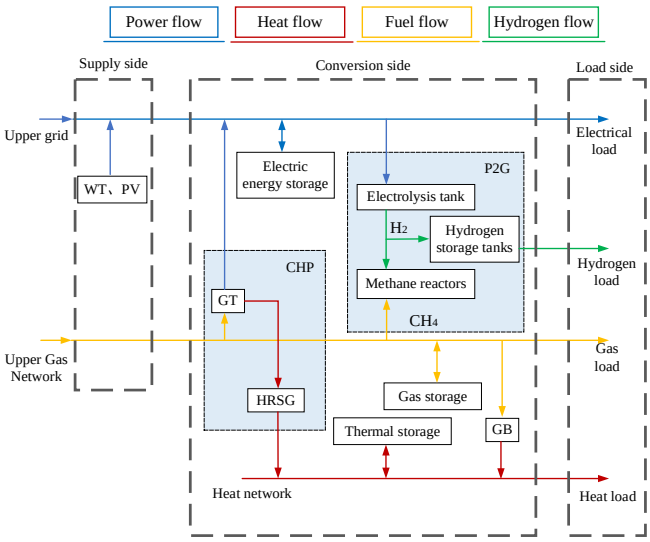

Fig. 1. VPP structure

III. Single Unit Models Involved in Optimal Scheduling of the VPP

A. Model of power supply equipment

Distributed wind and photovoltaic resources are clean energy sources, and the amount of carbon emissions they produce can be successfully reduced, which is more in line with the low carbon goals of this article, the power supply equipment in this paper mainly includes wind turbines and PV units.

(1) Wind turbine generation

The output formula is as follows:

$$P_{\mathrm{WT}}(t)=\begin{cases}0 & v\le v_{in}\\ av^3+bv^2+cv+d & v_{in}\le v\le v_e\\ P_e & v_e\le v\le v_{out}\\ 0 & v\ge v_{out}\end{cases} \tag{1}$$

Where the output power of the wind turbine is denoted as $P_{\mathrm{WT}}(t)$; P_e refers to the rated power of the wind turbine; v_e refers to the rated wind speed; v_{in} refers to cut-in wind speed; v_{out} stands for the cut-off wind speed; and a, b, c and d are coefficients.

(2) Photovoltaic (PV) power generation

The power output is modelled as follows:

$$P_{\mathrm{PV}}(t)=\lambda\cdot\rho_{\mathrm{PV}}\cdot\varphi(t) \tag{2}$$

where the PV unit's output power is denoted as $P_{\mathrm{PV}}(t)$; The PV panels' conversion efficiency is denoted by the λ, while their total area is denoted by the ρ_{PV} ; and φ(t) is the illumination intensity during period t.

B. Model of heating equipment

(1) Combined heat and power (CHP)

There are two components of a CHP unit: a gas turbine (GT) and a heat recovery steam generator (HRSG), which is mathematically modelled as follows:

$$P_{\mathrm{GT}}^{\mathrm{ele}}(t)=\frac{Q_{\mathrm{GT}}(t)L_{\mathrm{gas}}}{\Delta t}\eta_{\mathrm{GT}} \tag{3}$$

$$P_{\mathrm{HRSG}}^{\mathrm{heat}}(t)=\frac{P_{\mathrm{GT}}^{\mathrm{ele}}(t)(1-\eta_{\mathrm{GT}}-\eta_q)}{\eta_{\mathrm{GT}}}K_{\mathrm{HRSG}}^{\mathrm{he}}M_{\mathrm{HRSG}}^{\mathrm{sr}} \tag{4}$$

$$H_{\mathrm{HRSG}}(t)=P_{\mathrm{HRSG}}^{\mathrm{heat}}(t)\Delta t \tag{5}$$

where $P_{GT}^{ele}(t)$ and $Q_{GT}(t)$ refer to the output electric power and the GT's volumetric consumption of NG; L_{gas} refers to the low calorific value of NG; the thermal power output and the heat output value of HRSG are denoted as $P_{\mathrm{HRSG}}^{\mathrm{heat}}(t)$ and $H_{\mathrm{HRSG}}(t)$; η_{GT} refers to GT's power generation efficiency ; η_q refers to the heat dissipation loss rate of the HRSG; K_{HRSG}^{he} and M_{HRSG}^{sr} are the heating coefficient and flue gas recovery rate of the bromine cooler, respectively; and Δt is the unit scheduling period.

(2) Gas boiler (GB)

A GB is a type of energy conversion equipment that produces heat by consuming natural gas. A commonly used mathematical model expression is

$$P_{\mathrm{GB}}^{\mathrm{heat}}(t)=\frac{Q_{\mathrm{GB}}(t)L_{\mathrm{gas}}}{\Delta t}\eta_{\mathrm{GB}} \tag{6}$$

$$H_{\mathrm{GB}}(t)=P_{\mathrm{GB}}^{\mathrm{heat}}(t)\Delta t \tag{7}$$

where the GB's output thermal power is denoted as $P_{GB}^{heat}(t)$; the NG flow consumed by the GB is denoted as $Q_{GB}(t)$; $H_{GB}(t)$ refers to the heat generated by the GB; and η_{GB} refers to the gas heat conversion efficiency of the GB.

C. Model of energy storage equipment

(1) Electricity storage (ES)

Electricity storage (ES) can effectively overcome the shortcomings of clean energy output volatility. The specific mathematical model is as follows:

$$\begin{aligned}E_{\mathrm{ES}}(t+1)=(1-\delta^{\mathrm{ES}})E_{\mathrm{ES}}(t)+[\eta_{\mathrm{ES}}^{\mathrm{store}}P_{\mathrm{ES}}^{\mathrm{store}}(t+1)\\ -P_{\mathrm{ES}}^{\mathrm{release}}(t+1)/\eta_{\mathrm{ES}}^{\mathrm{release}}]\Delta t\end{aligned} \tag{8}$$

Where the charging and discharging powers of the ES system are denoted as $P_{ES}^{store}(t)$ and $P_{ES}^{release}(t)$, respectively; η_{ES}^{store} refers to the charging efficiency of the ES ; $\eta_{ES}^{release}$ refers to discharging efficiency of the ES system; δ^{ES} is the self-loss rate of the ES system; the storage capacities of the ES system are denoted as $E_{ES}(t)$.

(2) Heat storage (HS)

The specific mathematical model is as follows:

$$\begin{aligned}H_{\mathrm{HS}}(t+1)=(1-\delta^{\mathrm{HS}})H_{\mathrm{HS}}(t)+[\eta_{\mathrm{HS}}^{\mathrm{store}}P_{\mathrm{HS}}^{\mathrm{store}}(t+1)\\ -P_{\mathrm{HS}}^{\mathrm{release}}(t+1)/\eta_{\mathrm{HS}}^{\mathrm{release}}]\Delta t\end{aligned} \tag{9}$$

where $P_{HS}^{store}(t)$ and $P_{HS}^{release}(t)$ are the heat storage and heat release power of the HS system during period t, respectively; η_{HS}^{store} refers to heat storage efficiency of the HS system; $\eta_{HS}^{release}$ refers to heat release efficiency of the HS system; δ^{HS} refers to self-loss rate of the HS system; and $H_{HS}(t)$ and $H_{HS}(t-1)$ stand for the heat storage of the HS system, respectively.

(3) Gas storage (GS)

The specific mathematical model is as follows:

$$\begin{aligned}Q_{\mathrm{GS}}(t+1)=(1-\delta^{\mathrm{GS}})Q_{\mathrm{GS}}(t)+[\eta_{\mathrm{GS}}^{\mathrm{store}}P_{\mathrm{GS}}^{\mathrm{store}}(t+1)/L_{\mathrm{gas}}\\ -P_{\mathrm{GS}}^{\mathrm{release}}(t+1)/(\eta_{\mathrm{GS}}^{\mathrm{release}}L_{\mathrm{gas}})]\Delta t\end{aligned} \tag{10}$$

where $P_{GS}^{store}(t)$ and $P_{GS}^{release}(t)$ refer to gas storage and bleeding power of the GS system; η_{GS}^{store} and $\eta_{GS}^{release}$ refer to gas storage efficiency and gas discharge efficiency of GS system, respectively; δ^{GS} is the self-loss rate of the GS system; and $Q_{GS}(t)$ refers to NG volumes stored by the GS system during periods t, respectively.

D. Model of power-to-gas equipment

(1) Power to gas (P2G)

There are two types of P2G equipment: one converts electric energy into hydrogen with an efficiency of 75%–85%, and the other converts hydrogen into electric energy into natural gas with an efficiency of 45%–60% through methanation. A two-step chemical equation is shown in Equation (11).

$$\begin{cases}2H_2O\xrightarrow{\text{electrolysis}}2H_2+O_2\\ CO_2+4H_2\xrightarrow{\text{catalyst}}CH_4+2H_2O\end{cases} \tag{11}$$

A traditional P2G system produces natural gas by methanating all the hydrogen generated by water electrolysis,

and if there is a demand for hydrogen load in the system, it is purchased from the higher gas network, which not only reduces safety but also prevents efficient P2G use. This paper considers the high efficiency of an initial electricity-to-hydrogen process and the developing trend of a hydrogen energy demand in the future; the two factors are combined to draw a two-stage P2G operation process, as shown in Figure 2. The first stage is the hydrogen energy generation stage, where the wind power that may originally be discarded through rectification flows into the electrolyser through the electrolysis of water to convert electrical energy. The electrolyser converts electricity into hydrogen energy by water electrolysis, and at the same time, to improve operational flexibility, hydrogen energy is stored in additional storage tanks to supply hydrogen. The second stage is the consumption of hydrogen energy, and if there is any surplus hydrogen, it is fed into the methane reactor and converted into CH_4. This is used by the CHP and the GB, thus not only achieving an efficient use of energy but also reducing risk when purchasing and transporting hydrogen, thus achieving a win–win situation.

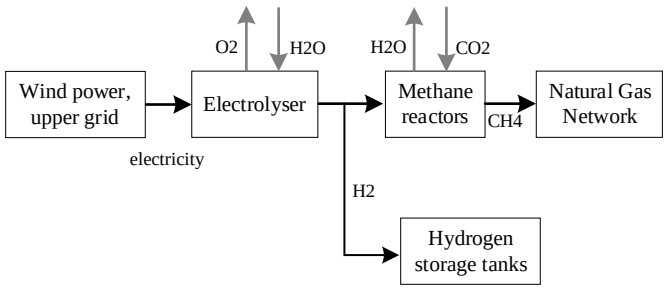

Fig. 2. Two-stage P2G operation process

A conventional P2G conversion process produces natural gas by consuming electrical energy to meet demand of the system. The power output is modelled as Equation (12-13):

$$P_{\mathrm{P2G}}^{\mathrm{gas}}(t)=P_{\mathrm{P2G}}^{\mathrm{ele}}(t)\eta_{\mathrm{P2G}} \tag{12}$$

$$Q_{\mathrm{P2G}}(t)=\frac{P_{\mathrm{P2G}}^{\mathrm{gas}}(t)\Delta t}{L_{\mathrm{gas}}} \tag{13}$$

where the NG power output and the electric power consumed by the P2G system are denoted as $P_{\mathrm{P2G}}^{\mathrm{gas}}(t)$ and $P_{\mathrm{P2G}}^{\mathrm{ele}}(t)$; $Q_{\mathrm{P2G}}(t)$ refers to the NG volume generated by the P2G system during period t; and η_{P2G} refers to electrical conversion efficiency of the P2G process.

(2) Electrolyser

The electrolyser can convert electrical energy into hydrogen by the electrolysis of water, the mathematical model of which is shown in Equation (14).

$$P_{\mathrm{EC}}=\eta_{\mathrm{EC}}P_{\mathrm{ECi}} \tag{14}$$

where P_{EC} and P_{ECi} are the output power and input power of the electrolyser, respectively; and η_{EC} refers to conversion efficiency of the electrolyser.

(3) Methane reactor

Hydrogen reacts with CO_2 in a methane reactor via the Sabatier process to form CH_4 and water, where the mathematical model of the methane reactor is shown in Equation (15).

$$P_{\mathrm{MR}}=\eta_{\mathrm{MR}}P_{\mathrm{MRi}} \tag{15}$$

where P_{MR} and P_{MRi} are the output power and input power of the methane reactor during period t, respectively, and η_{MR} refers to the conversion efficiency of the methane reactor.

(4) Hydrogen storage tank

The model is shown in Equation (16).

$$E_{\mathrm{HST,t}}=E_{\mathrm{HST,t\text{-}1}}+\eta_{\mathrm{HSTi,t}}P_{\mathrm{HSTi,t}}-\frac{P_{\mathrm{HSTo,t}}}{\eta_{\mathrm{HSTo}}} \tag{16}$$

where $E_{\mathrm{HST,t}}$ refers to capacity of the hydrogen storage tank; the input and output power of the hydrogen storage tank are denoted as P_{HSTi} and P_{HSTo} during period t, respectively; η_{HSTi} and η_{HSTo} refer to hydrogen storage efficiency and hydrogen release efficiency.

E. Integrated demand response load

With the increase in flexible loads such as electric vehicles and inverter air conditioners on the energy consumption side, it is increasingly important to study demand response loads to improve the flexible operation of integrated energy systems. It is characterised by the fact that the total amount of load and the amount of load in each time period is not constant during the dispatch time. Within the defined time period and the amount of load, the demand response load can be shifted, reduced and substituted to achieve the desired requirements by processing the different transgressive loads. In general, demand response loads can be shifted, curtailable or substitutable loads. In this paper, only thermal loads are replaced by electrical loads. The specific model is as follows:

$$P_{\mathrm{load}}(t)=P_{\mathrm{load}}^{'}(t)+P_{\mathrm{load}}^{\mathrm{cut}}(t)+P_{\mathrm{load}}^{\mathrm{tran}}(t)+P_{\mathrm{load}}^{\mathrm{rep}}(t) \tag{17}$$

$$H_{\mathrm{load}}(t)=H_{\mathrm{load}}^{'}(t)+H_{\mathrm{load}}^{\mathrm{cut}}(t)+H_{\mathrm{load}}^{\mathrm{tran}}(t)-P_{\mathrm{load}}^{\mathrm{rep}}(t) \tag{18}$$

$$-P_{\mathrm{load,max}}^{\mathrm{cut}}(t)\le -P_{\mathrm{load}}^{\mathrm{cut}}(t)\le 0 \tag{19}$$

$$\sum_{t=1}^{T}P_{\mathrm{load}}^{\mathrm{tran}}(t)\Delta t=0,\quad \left|P_{\mathrm{load}}^{\mathrm{tran}}(t)\right|\le P_{\mathrm{load,max}}^{\mathrm{tran}}(t) \tag{20}$$

where $P_{\mathrm{load}}(t)$, $P'_{\mathrm{load}}(t)$, $H_{\mathrm{load}}(t)$ and $H'_{\mathrm{load}}(t)$ refer to the electrical load demand value, predicted value of electrical load demand, thermal load demand value and predicted value of thermal load demand of the VPP, respectively; $P_{\mathrm{load}}^{\mathrm{cut}}(t)$, $P_{\mathrm{load}}^{\mathrm{tran}}(t)$ and $P_{\mathrm{load}}^{\mathrm{rep}}(t)$ are the reducible, transferable and replaceable electrical loads of the VPP system, respectively; $H_{\mathrm{load}}^{\mathrm{cut}}(t)$ and $H_{\mathrm{load}}^{\mathrm{tran}}(t)$ are the reducible and transferable heat loads; and the maximum values of the reducible and transferable electrical loads are denoted as $P_{\mathrm{load,max}}^{\mathrm{cut}}(t)$ and $P_{\mathrm{load,max}}^{\mathrm{tran}}(t)$.

IV. Economic Optimal Dispatch Model for VPPs

A. Target function

To achieve economic optimisation and minimise carbon emissions, we transform a multiobjective problem into a single-objective optimisation problem by introducing a carbon tax c_{tax}, which converts carbon emissions into carbon costs. With the objective function of minimising the sum of

the operating cost C_1 and the carbon emission cost C_2 of the VPP in the park, the optimisation objective is established as follows:

$$\begin{cases} \min C = C_1 + C_2 \\ C_1 = \sum_{t=1}^{24} [(C_{\mathrm{G}} + C_{\mathrm{IDR}} + C_{\mathrm{MAIN}} + C_{\mathrm{GRID}})] \\ C_2 = c_{\mathrm{tax}} \sum_{t=1}^{24} (e_{\mathrm{CHP}} + e_{\mathrm{GB}}) \end{cases} \quad (21)$$

where C_{G}, C_{IDR}, C_{MAIN} and C_{GRID} are the system energy purchase costs, compensation costs for demand-side response load, the expense of each unit's equipment upkeep and the interaction cost of purchasing and selling electricity with the superior power grid, respectively, and e_{CHP} and e_{GB} are the carbon emission cost of CHP and the gas-fired boiler, respectively.

(1) Operating cost C_1

1) System energy purchase costs

There are a number of devices that require electricity and NG to start them up, so the system of VPP requires the purchase of external energy to meet the operating needs. The cost can be expressed as Equation (22):

$$C_{\mathrm{G}} = \left[f_{\mathrm{BG}}(t) P_{\mathrm{BG}}(t) + f_{\mathrm{gas}}(t) Q_{\mathrm{BG}}(t) \right] \Delta t \quad (22)$$

where $f_{\mathrm{BG}}(t)$ and $f_{\mathrm{gas}}(t)$ refer to the unit prices when the system purchases electricity from the upper grid and NG from the superior gas network in period t, $Q_{\mathrm{BG}}(t)$ is the external natural gas volume purchased by the system during period t, and Δt is the unit scheduling period.

2) Compensation costs for demand-side response load volumes

$$\begin{aligned} C_{\mathrm{IDR}} = (& f_{\mathrm{cut}}^{\mathrm{ele}} \left| P_{\mathrm{load}}^{\mathrm{cut}}(t) \right| + f_{\mathrm{tran}}^{\mathrm{ele}} \left| P_{\mathrm{load}}^{\mathrm{tran}}(t) \right| \\ & + f_{\mathrm{rep}}^{\mathrm{ele}} \left| P_{\mathrm{load}}^{\mathrm{rep}}(t) \right| + f_{\mathrm{cut}}^{\mathrm{heat}} \left| H_{\mathrm{load}}^{\mathrm{cut}}(t) \right| \\ & + f_{\mathrm{tran}}^{\mathrm{heat}} \left| H_{\mathrm{load}}^{\mathrm{tran}}(t) \right|) \Delta t \end{aligned} \quad (23)$$

where $f_{\mathrm{cut}}^{\mathrm{ele}}$, $f_{\mathrm{tran}}^{\mathrm{ele}}$ and $f_{\mathrm{rep}}^{\mathrm{ele}}$ refer to reducible, transferable and replaceable electric loads' unit compensation cost coefficients, respectively; $f_{\mathrm{cut}}^{\mathrm{heat}}$ and $f_{\mathrm{tran}}^{\mathrm{heat}}$ refer to unit compensation cost coefficients of the heat load that can be reduced and transferred, respectively; $P_{\mathrm{load}}^{\mathrm{cut}}(t)$, $P_{\mathrm{load}}^{\mathrm{tran}}(t)$ and $P_{\mathrm{load}}^{\mathrm{rep}}(t)$ are the reducible, transferable and replaceable electrical loads of the system during period t, respectively; the reducible, transferable heat loads are denoted as $H_{\mathrm{load}}^{\mathrm{cut}}(t)$ and $H_{\mathrm{load}}^{\mathrm{tran}}(t)$, respectively.

3) Maintenance costs for each unit in the system

Each unit incurs corresponding maintenance costs during the operation of the system. Maintenance costs vary from unit to unit. The maintenance cost is as follows:

$$\begin{aligned} C_{\mathrm{MAIN}} = [& f_{\mathrm{PV}}(t) P_{\mathrm{PV}}(t) + f_{\mathrm{WT}}(t) P_{\mathrm{WT}}(t) \\ & + f_{\mathrm{CHP}} (P_{\mathrm{GT}}^{\mathrm{ele}}(t) + P_{\mathrm{HRSG}}^{\mathrm{heat}}(t)) \\ & + f_{\mathrm{GB}} P_{\mathrm{GB}}^{\mathrm{heat}}(t) + f_{\mathrm{P2G}} P_{\mathrm{P2G}}^{\mathrm{gas}}(t) \\ & + f_{\mathrm{ES}} (P_{\mathrm{ES}}^{\mathrm{store}}(t) - P_{\mathrm{ES}}^{\mathrm{release}}(t)) \\ & + f_{\mathrm{HS}} (P_{\mathrm{HS}}^{\mathrm{store}}(t) - P_{\mathrm{HS}}^{\mathrm{release}}(t)) \\ & + f_{\mathrm{GS}} (P_{\mathrm{GS}}^{\mathrm{store}}(t) - P_{\mathrm{GS}}^{\mathrm{release}}(t))] \Delta t \end{aligned} \quad (24)$$

where f_{PV}, f_{WT}, f_{CHP}, f_{GB}, f_{P2G}, f_{ES}, f_{HS} and f_{GS} are the corresponding unit maintenance costs of the PV unit, wind turbine unit, CHP system, GB, P2G system, and energy storage device, respectively.

4) Interaction costs between the system and the higher-level grid

The demand for electricity in industrial parks is generally large, while scenic power units generally have limited and uncertain installed capacities. Therefore, in the processes of system optimisation and control, if the power supply through the wind power output is insufficient, it needs to buy power from the superior grid. Combining actual peak and valley tariffs and the operating characteristics of the CHP, P2G, EB and ES systems, the levels of interaction between the systems and the upper grid can be further improved. In addition, if the system produces excess power, it can also be sold to the higher power grid, thus reducing the system operating costs. The cost of the system's interaction with the parent grid is as follows:

$$C_{\mathrm{GRID}} = [f_{\mathrm{BG}}(t) P_{\mathrm{BG}}(t) - f_{\mathrm{SG}}(t) P_{\mathrm{SG}}(t)] \Delta t \quad (25)$$

where the power purchase price and power sale price are denoted as $f_{\mathrm{BG}}(t)$ and $f_{\mathrm{SG}}(t)$, respectively; $P_{\mathrm{BG}}(t)$ and $P_{\mathrm{SG}}(t)$ refer to the power purchased and sold to the superior power grid during period t.

(2) Cost of carbon emissions C_2

The cost of carbon emissions consists of two parts: the cost of carbon emissions from the CHP system (e_{CHP}) and the GB system (e_{GB}), where e_{CHP} is the difference between the CHP unit carbon emissions c_{CHP} and the carbon emission allowances c_{CHPb}.

$$\begin{cases} e_{\mathrm{CHP}} = c_{\mathrm{CHP}} - c_{\mathrm{CHPb}}, \\ e_{\mathrm{GB}} = \mu_{\mathrm{GB}} P_{\mathrm{GBh}} \end{cases} \quad (26)$$

$$\begin{cases} P_{\mathrm{CHP}} = P_{\mathrm{CHPe}} + \gamma P_{\mathrm{CHPh}}, \\ c_{\mathrm{CHP}} = \sum_{t=1}^{24} (\alpha_1 P_{\mathrm{CHP}}^2 + \alpha_2 P_{\mathrm{CHP}} + \alpha_3) \\ c_{\mathrm{CHPb}} = \beta \sum_{t=1}^{24} P_{\mathrm{CHP}} \end{cases} \quad (27)$$

where the unit CO_2 emission cost of the GB is denoted as μ_{GB}; The electric power of the CHP unit transformed to the pure condensing condition at period t is indicated by the symbol P_{CHP}; γ refers to reduction value of the electric power when the CHP unit increases the unit thermal power under fixed air intake; α_1, α_2, and α_3 refers to the carbon emission

coefficients of CHP; the carbon trading quota per unit of electricity is denoted as β.

B. Constraint condition

(1) Power balance constraint

Power balance, heat balance and gas balance constraints need to be met in the scheduling and operation of the park's VPP.

$$\begin{cases} P_{\text{load}}(t) = P_{\text{PV}}(t) + P_{\text{WT}}(t) + P_{\text{GT}}^{\text{ele}}(t) \\ \qquad - P_{\text{P2G}}^{\text{ele}}(t) + P_{\text{BG}}(t) - P_{\text{SG}}(t) \\ \qquad + P_{\text{ES}}^{\text{release}}(t) - P_{\text{ES}}^{\text{store}}(t) \\ H_{\text{load}}(t) = H_{\text{HRSG}}(t) + H_{\text{GB}}(t) \\ \qquad + H_{\text{HS}}(t-1) - H_{\text{HS}}(t) \\ Q_{\text{load}}(t) = Q_{\text{BG}}(t) + Q_{\text{P2G}}(t) - Q_{\text{GB}}(t) \\ \qquad - Q_{\text{GT}}(t) + Q_{\text{GS}}(t-1) - Q_{\text{GS}}(t) \end{cases} \tag{28}$$

where the electrical load, thermal load and gas load are denoted as $P_{\text{load}}(t)$, $H_{\text{load}}(t)$ and $Q_{\text{load}}(t)$, respectively; $P_{\text{BG}}(t)$ and $P_{\text{SG}}(t)$ refer to the power purchased and sold from the superior power grid, respectively; $P_{\text{ES}}^{\text{release}}(t)$ and $P_{\text{ES}}^{\text{store}}(t)$ are the discharging power and the charging power of ES during period t; $H_{\text{HS}}(t)$ refers to the heat storage of the HS system during periods t; $Q_{\text{BG}}(t)$ and $Q_{\text{P2G}}(t)$ are the amounts of external NG purchased by the system and NG generated by the P2G system, respectively; and the gas storage capacity of the GS system is denoted as $Q_{\text{GS}}(t)$.

(2) System interaction constraints with the higher-level master network

When the power within the VPP is higher or lower than the load, the power balance can be ensured through power interactions with the public grid for power purchase and sale and between VPPs, and when considering the power interactions and demand response between VPPs, the power exchange with the public grid can be reduced, thus reducing the overall operating costs of the VPP. In order to reduce the regulation pressure on the upper mains network, this paper only takes into account the system's energy purchase from the upper mains network without considering energy sales.

$$\begin{cases} P_{\text{B}\min}(t) \le P_{\text{BG}}(t) \le P_{\text{B}\max}(t) \\ P_{\text{S}\min}(t) \le P_{\text{SG}}(t) \le P_{\text{S}\max}(t) \\ Q_{\text{B}\min}(t) \le Q_{\text{BG}}(t) \le Q_{\text{B}\max}(t) \end{cases} \tag{29}$$

where the minimum and maximum power limits for the system to purchase power from the superior grid are denoted as $P_{\text{Bmin}}(t)$ and $P_{\text{Bmax}}(t)$; $P_{\text{Smin}}(t)$ and $P_{\text{Smax}}(t)$ refer to the minimum and maximum power limits for the system to sell electricity to the upper grid, respectively; and $Q_{\text{Bmin}}(t)$ and $Q_{\text{Bmax}}(t)$ refer to the upper and lower limit of interaction between the superior gas network and the system during period t, respectively.

(3) Unit equipment constraints

$$\begin{cases} P_{\text{GTmin}}(t) \le P_{\text{GT}}^{\text{ele}}(t) \le P_{\text{GT}\max}(t) \\ P_{\text{GBmin}}(t) \le P_{\text{GB}}^{\text{heat}}(t) \le P_{\text{GB}\max}(t) \\ P_{\text{P2Gmin}}(t) \le P_{\text{P2G}}^{\text{gas}}(t) \le P_{\text{P2G}\max}(t) \end{cases} \tag{30}$$

$$\begin{cases} -R_{\text{GT}}^{\text{down}}\Delta t \le P_{\text{GT}}^{\text{ele}}(t) - P_{\text{GT}}^{\text{ele}}(t\text{-}1) \le R_{\text{GT}}^{\text{up}}\Delta t \\ -R_{\text{GB}}^{\text{down}}\Delta t \le P_{\text{GB}}^{\text{heat}}(t) - P_{\text{GB}}^{\text{heat}}(t\text{-}1) \le R_{\text{GB}}^{\text{up}}\Delta t \\ -R_{\text{P2G}}^{\text{down}}\Delta t \le P_{\text{P2G}}^{\text{gas}}(t) - P_{\text{P2G}}^{\text{gas}}(t\text{-}1) \le R_{\text{P2G}}^{\text{up}}\Delta t \end{cases} \tag{31}$$

where the minimum and maximum output electric powers of GT are denoted as $P_{\text{GTmin}}(t)$ and $P_{\text{GTmax}}(t)$, respectively; the minimum and maximum values of the output power of GB are denoted as $P_{\text{GBmin}}(t)$ and $P_{\text{GBmax}}(t)$; the minimum and maximum values of the output NG power of P2G are denoted as $P_{\text{P2Gmin}}(t)$ and $P_{\text{P2Gmax}}(t)$; $R_{\text{GT}}^{\text{up}}$ and $R_{\text{GT}}^{\text{down}}$ are upper and lower climbing speed limits of the GT system, respectively; $R_{\text{GB}}^{\text{up}}$ and $R_{\text{GB}}^{\text{down}}$ are the upper and lower climbing speed limits of the GB system, respectively; and the upper and lower climbing speed limit of P2G are denoted as $R_{\text{P2G}}^{\text{up}}$ and $R_{\text{P2G}}^{\text{down}}$.

(4) Energy storage equipment constraints

$$\begin{cases} E_{\text{ES}}^{\min} \le E_{\text{ES}}(t) \le E_{\text{ES}}^{\max} \\ H_{\text{HS}}^{\min} \le H_{\text{HS}}(t) \le H_{\text{HS}}^{\max} \\ Q_{\text{GS}}^{\min} \le Q_{\text{GS}}(t) \le Q_{\text{GS}}^{\max} \end{cases} \tag{32}$$

$$\begin{cases} 0 \le P_{\text{store}}(t) \le S_{\text{s}}(t) P_{\text{s}\max} \\ 0 \le P_{\text{release}}(t) \le S_{\text{r}}(t) P_{\text{r}\max} \end{cases} \tag{33}$$

$$\begin{cases} S_{\text{s}}(t) = \{0,1\} \\ S_{\text{r}}(t) = \{0,1\} \end{cases} \tag{34}$$

$$0 \le S_{\text{s}}(t) + S_{\text{r}}(t) \le 1 \tag{35}$$

where $E_{\text{ES}}^{\min}$, $E_{\text{ES}}^{\max}$, $H_{\text{HS}}^{\min}$, $H_{\text{HS}}^{\max}$, $Q_{\text{GS}}^{\min}$ and $Q_{\text{GS}}^{\max}$ refer to minimum and maximum capacities of ES, HS, and GS, respectively; $P_{\text{store}}(t)$ and $P_{\text{release}}(t)$ refer to charging and discharging powers of ES; the upper limits of the charging and discharging power of ES are denoted as P_{smax} and P_{rmax}, respectively; the charging and discharging states of ES are denoted as $S_{\text{s}}(t)$ and $S_{\text{r}}(t)$ during period t, respectively; and 1 and 0 indicate that ES is in the charging and discharging states or the noncharging and discharging states, respectively.

V. Example Analysis

A. Basic data

The VPP is designed to consist of wind turbines, PV units, cogeneration units, GBs, and ES devices aggregated together, and an industrial park is selected for the research. A dispatch cycle is set as 24 h, and a unit dispatch period is set as 1 h. In this example, the low calorific value of natural gas is 9.7 kWh/m^3, and GHV is 35.54 MJ/m^3. The wind-power prediction curves for a typical day is shown in Figure 3 , and the electrical, thermal and gas load forecasting curves is shown in Figure 4.

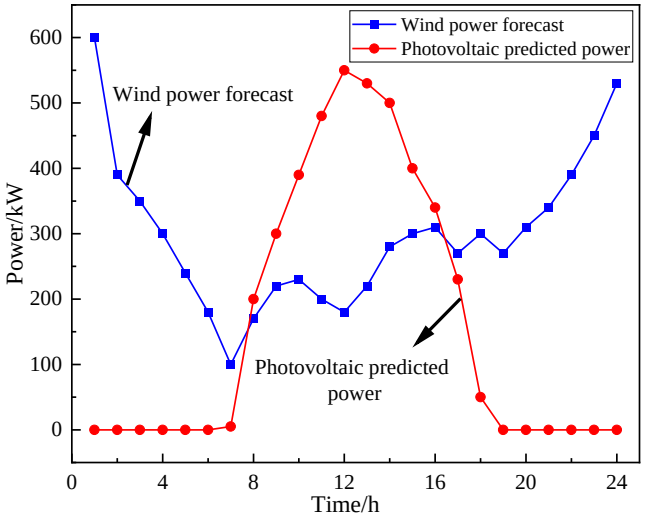

Fig. 3. Typical daily wind and light power prediction curve

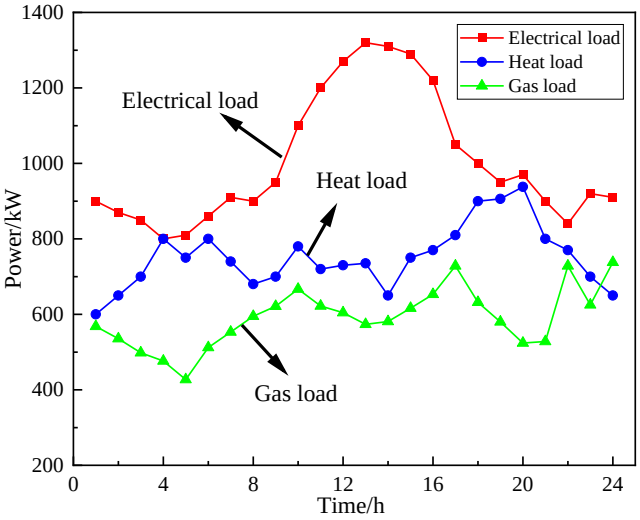

Fig. 4. Typical electric, heat and gas load forecasting curve

TABLE I
EQUIPMENT PARAMETERS

Type of equipment	Minimum output power (kW)	Maximum output power (kW)	Efficiency	Maintenance costs (yuan/kWh)
CHP	0	1000	0.45	0.15
GB	300	600	0.85	0.18
P2G	300	600	0.6	0.15

TABLE II
PARAMETERS OF ENERGY STORAGE EQUIPMENT

Type of equipment	Maximum power for charging (kW)	Maximum power of discharging (kW)	Self-consumption rate of equipment	Maintenance costs (yuan/kWh)
ES	300	400	0.01	0.018
HS	600	700	0.05	0.016
GS	500	600	0.02	0.017

TABLE III
DEMAND RESPONSE LOAD COMPENSATION PRICE

Type of load	Cost (yuan/kWh)
Transferable electrical/heat load	0.16
Reducible electrical/heat load	0.14
Substitutable electrical load	0.12

In the example, the unit maintenance costs of wind power and PV units are both taken as 0.23 yuan/kWh. In the cost of carbon emissions, a_1, a_2 and a_3 are taken as 0.0532, 190.12 and 13175.4, respectively. γ is taken as 0.15, and β is taken as 0.798. The technical parameters of each unit of equipment are shown in Tables I and II.

The compensation prices for the demand response loads in the example are shown in Table III. The system uses the local time-of-use tariff for the purchase and sale of electricity with the superior grid, with a peak hour purchase price of 0.95 yuan/kWh and a sale price of 0.54 yuan/kWh from 11:00–21:00, an ordinary hour purchase price of 0.65 yuan/kWh and a sale price of 0.47 yuan/kWh from 8:00–10:00 and 22:00–24:00, and a peak hour purchase price of 0.38 yuan/kWh and a sale price of 0.33 yuan/kWh from 1:00–7:00.

B. Scenario setting and analysis of result

To verify that VPP aggregated in this paper is more economical and clean, the following three scenarios are established to compare and analyse the system operation results under different scenarios.

Scenario 1: The VPP is operated in a conventional manner for a subsequent visual comparison with the VPP operation in Scenarios 2 and 3.

Scenario 2: Consideration of the electrical and thermal load demand responses based on Scenario 1

Scenario 3: Based on Scenario 2, the hydrogen obtained in the first stage of the P2G conversion process is stored in a storage tank to supply the load, and the remaining hydrogen is then subjected to a methanation reaction (i.e., the model

developed in this paper).

(1) Impacts of the VPP build method on costs

The simulation study of the VPP in this industrial park under the selected typical day under different scenarios allows the system operating costs for each scenario to be obtained, as shown in Table IV.

TABLE IV
EACH SCENARIO COST COMPARISON

Cost category/yuan	Scenario 1	Scenario 2	Scenario 3
Cost of system interaction with the parent grid/yuan	1608.1	458.6	634.7
System purchase of external gas cost/yuan	20536	20399	10711.4
Equipment maintenance cost/yuan	9352.8	9130.9	10562.5
Demand response load compensation cost/yuan	0	415	409.8
Cost of carbon emissions/yuan	5685.6	5632.8	5013.5
Total running costs/yuan	37182.5	36036.3	27331.9

According to the analysis in Table IV, since Scenario 1 is operated in a traditional manner without considering the integrated demand responses of electricity and heat and the two-stage P2G conversion process, the system purchases more energy and has the highest electricity purchase costs and sale interactions with the superior grid, but there is no demand response load compensation cost. On the basis of Scenario 1, Scenario 2 addresses the combined demand response for heat and electricity, so Scenario 2 has an additional demand response load compensation cost of $415 compared to Scenario 1. However, due to the addition of demand response loads, the baseline load decreases during peak periods, reducing the pressure on the generating units compared to scenarios where demand response is not considered, effectively relieving the internal load of the virtual power plant and making the system in Scenario 2 reduce the cost of electricity purchase and sale interaction with the superior grid by 70.5% compared to Scenario 1. Scenario 3 has the highest operation and maintenance cost because its two-stage electricity to gas equipment is considered compared to Scenario 2. Due to the operation of the electrolyser and other equipment, its purchased electricity cost is slightly higher, but the purchased gas cost is substantially lower, mainly due to the use of wind power to produce hydrogen, which provides a certain capacity of hydrogen for the system, and this method also reduces the danger in the process of transporting hydrogen and improves the efficiency of the multienergy coupling within the VPP. In addition, the total cost of Scenario 3 is reduced by 26.5% and 24.2% compared to Scenario 1 and Scenario 2, respectively, so the optimisation model proposed in this paper, i.e., Scenario 3 has better economics in the operation of the VPP.

(2) Analysis of the P2G operation

As seen in Figure 5, during the periods of 1:00–7:00 and 22:00–24:00, when wind power is high and the price of electricity is low, the P2G output is high, while during the other periods from 7:00 to 22:00, the wind power output decreases and the P2G output is basically nonexistent, converting electricity from the low-cost periods into other forms of energy to supply the load during the high-cost periods. The hydrogen produced in the electrolyser is fed into the methane reactor to produce natural gas to supply the gas load, and the hydrogen produced in most of the remaining hours is stored directly in the hydrogen storage tank to supply the hydrogen load, reducing the energy loss caused by multistage conversion compared to methanation again

.

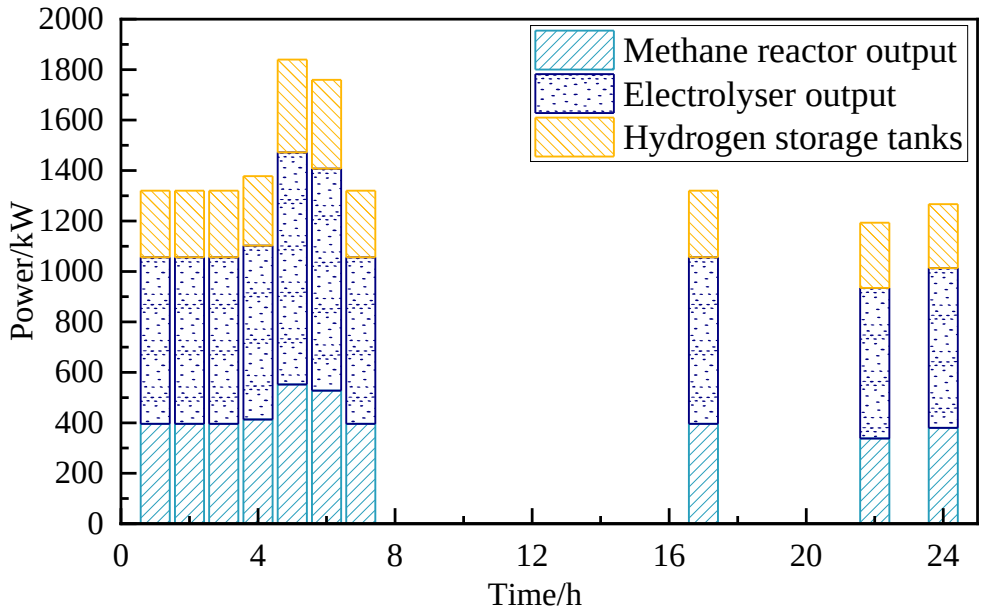

Fig. 5. Output of the electrolyser and the methane reactor

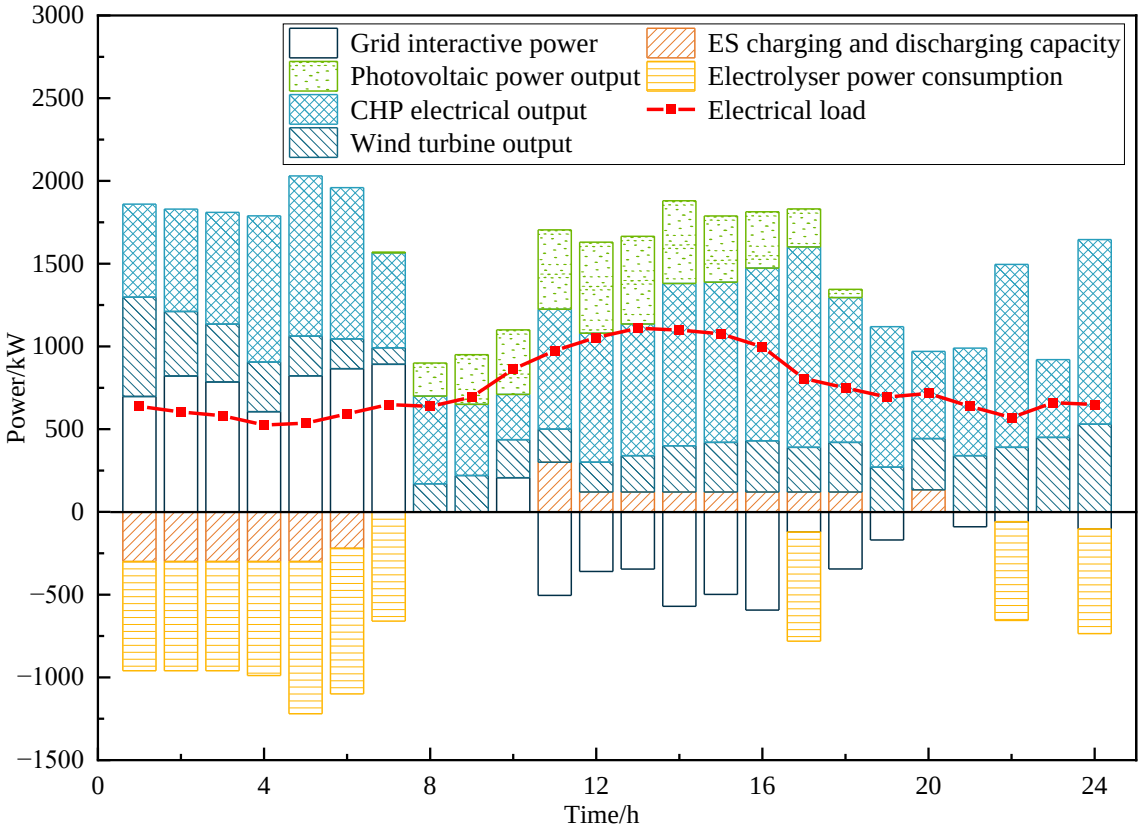

Fig. 6. Scenario 3 power balance operation result

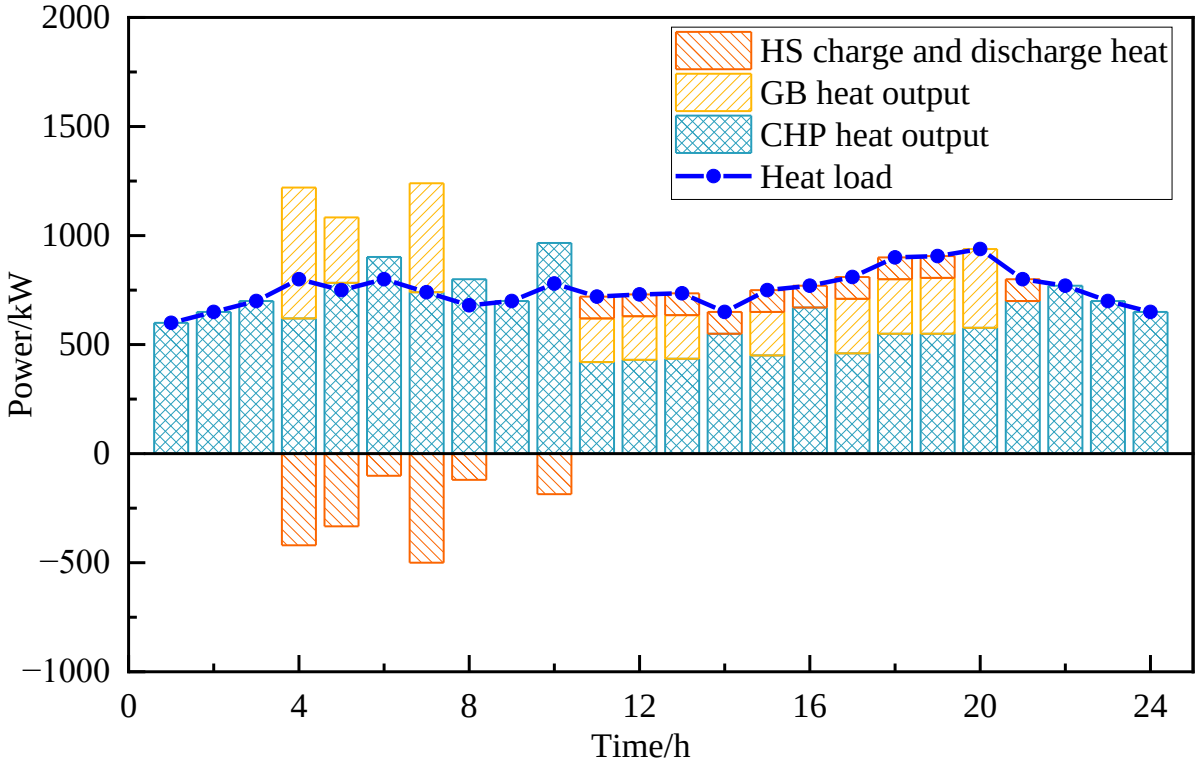

Fig. 7. Scenario 3 thermal balance operation result

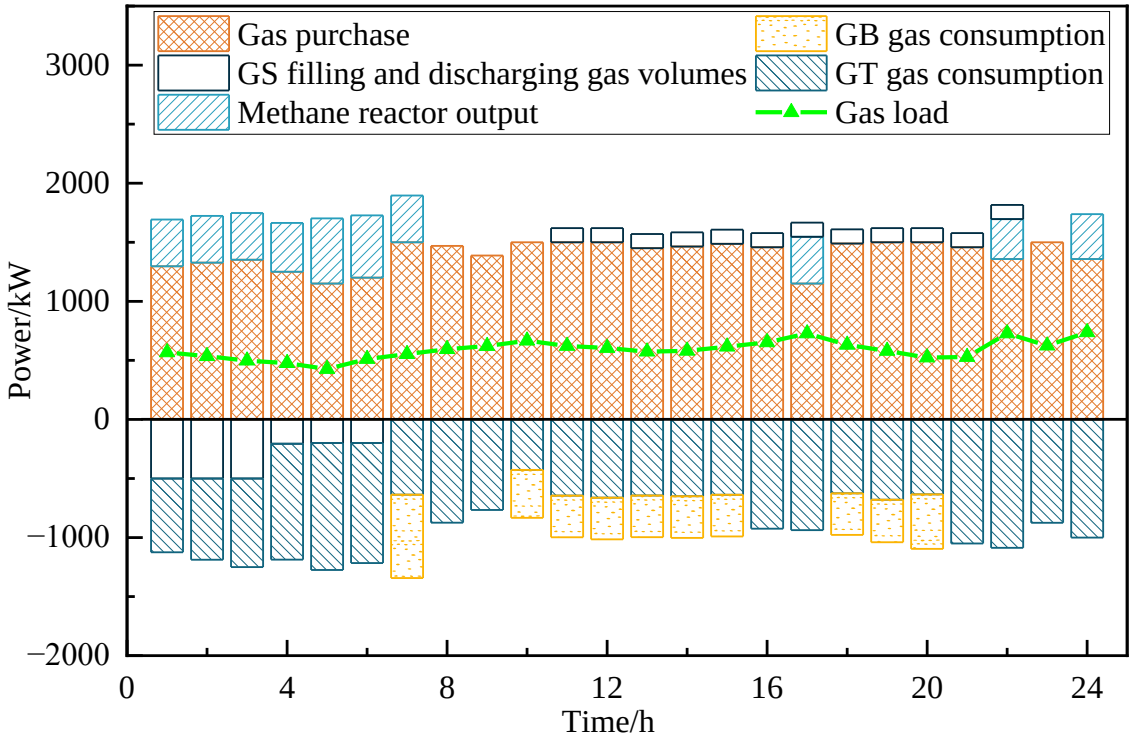

Fig. 8. Scenario 3 natural gas balance operation result

(3) Scheduling optimisation results analysis

Figures 6–8 show the results of the electricity balance, heat balance and gas balances under Scenario 3.

As seen in Figure 6, since the incorporated demand response of electricity and heat, as well as the two-stage P2G conversion process, are taken into account in Scenario3, the system load power demand is met at this time by the system's purchase of energy out from upper power system, the electrical power output of the CHP units, and the outputs of the wind and PV units. During the 1:00–7:00 and 22:00–24:00 periods, when wind power is abundant and electricity prices are low, the P2G conversion output is higher; however, during the other periods, the P2G conversion output is basically nonexistent, converting the electricity during the low-cost hours into other forms of energy to supply the load during the high-cost hours. This phenomenon reduces the system operating costs. As the wind turbines produce more power at night, the excess power is still stored by the ES system at this time. Since the PV unit output is higher during the day and the electrical load after the demand response is not much different from that at night, the system prioritises using the wind turbine generation during the daytime period to fully use the clean energy output. During the 11:00–21:00 period at the peak of the electricity tariff, the ES system is used to meet the electrical load demand by discharging.

The results of the system heat balance optimisation in Scenario 3 are shown in Figure 7. During the 1:00–7:00 period, the heat load demand is mainly met by the CHP output because it is at a low electricity price at this time; when the CHP system reaches its output limit, the GB output is used, and the excess heat generated is stored by the HS system. During the 8:00–10:00 period, the EB system has sufficient power input because the scenic units are out of power; thus, the EB system remains in working condition during this period. From 11:00–21:00, due to the higher electricity prices and the lower gas unit prices, the heat load demand is mainly met by the thermal power output of the CHP units and the GB output, while the HS system exerts heat, reducing the operating costs of the system.

The natural gas balance optimisation results in Scenario 3 are shown in Figure 8. The gas load demand is mainly met by the system purchasing external gas throughout the 24-hour day, while the CHP unit consumes more gas to output electrical and thermal energy to meet the electrical and thermal loads due to its low power output cost. When the system reaches its maximum purchase of gas from the upper grid, the output is supplemented by the GS system and methane reactors. During the period 1:00–7:00, when electricity prices are low, the methane reactor starts working and produces natural gas by consuming electricity, and the excess gas is stored by the GS system. During the hours of 11:00–21:00, when electricity prices are high, the methane reactor, which more expensively produces gas, stops working, and the gas load demand is mainly met by the system purchasing gas from external sources and by the GS bleeding gas. The various pieces of equipment work synergistically to reduce system operating costs.

(4) Sensitivity analysis

Different weights r_1 and r_2 are assigned to the system operating cost C_1 and the carbon emission cost C_2, respectively, as shown in Equation (40). Their impacts on the system are analysed. The weight coefficients are used to indicate the amount of attention being given, and $r_1 + r_2 = 1$. When $r_1 > r_2$, more attention is given to the system's operating cost, i.e., economy; when $r_1 < r_2$, more attention is given to the system's carbon emission cost, i.e., environmental friendliness. Figure 9 shows the variation curves of economic indicators, environmental indicators and the total costs for different weighting factors.

$$\min C^{'} = \lambda_1 C_1 + \lambda_2 C_2 \tag{36}$$

where C' is the total cost after adding the weighting factor.

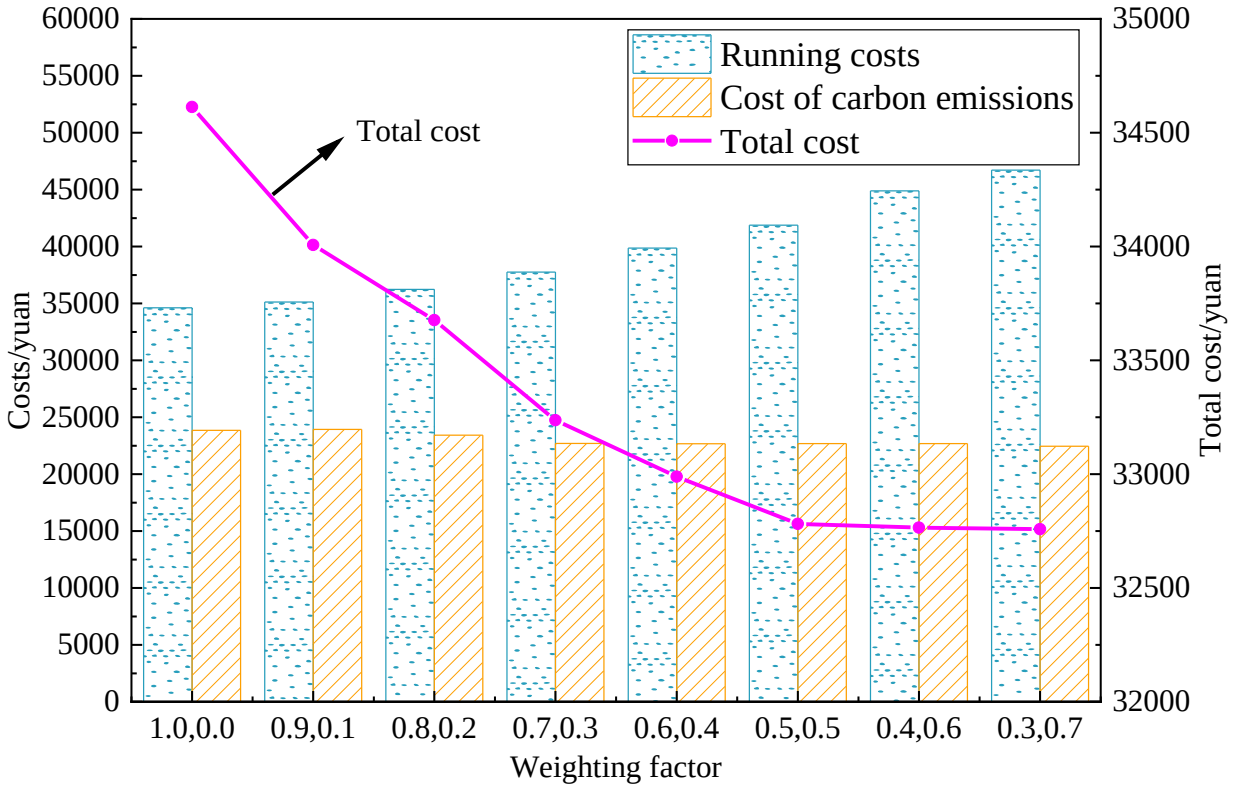

Fig. 9 Comparison of indicators under different weight coefficients

Different coefficient settings affect the final optimisation results: When r_2 is large, decision-makers pay more attention to environmental protection, the carbon emission cost decreases, and the operating cost significantly increases, and vice versa. Figure 9 shows that when the weight coefficient changes from extreme attention to economic benefits (r_1=1, r_2=0) to slight attention to economic benefits (r_1=0.7, r_2=0.3), with the reduction in attention to the economy, the operating cost increases, and the carbon emission cost decreases. However, paying excessive attention to carbon emissions leads to a significant increase in operating costs; at this time, the reduction in carbon emissions is very limited. Therefore, the coefficient range on the right side of the coordinate axis has no actual reference value, and the cost performance is very low. In summary, the ranges of reasonable coefficients are as follows: (r_1=0.7, r_2=0.3) ~ (r_1=0.4, r_2=0.6).

VI. Conclusion

In this paper, by introducing the multienergy coupled operation of power-to-gas and virtual power plants with internal CHP units and gas turbines and constructing a model for the optimal dispatch operation of participating VPPs, with the objective of minimising the sum of operating costs and carbon emission costs, combined with arithmetic simulations, the following conclusions are drawn.

(1) The electrolyser, methane reactor and hydrogen storage tank constitute the mutual coupling between electricity, hydrogen and natural gas within the virtual power plant, fully considering the difference in conversion efficiency between the two stages of P2G and taking into account the future development trend of integrated energy systems, converting wind energy into hydrogen required by the system, reducing the energy loss caused by step conversion; To a certain extent, through energy transfer, the load demand of the virtual power plant system in the period of high cost is met, the economic goal is achieved, and the energy utilization rate and low-carbon cleanliness are improved.

(2) In the coordinated electricity-heat-gas optimal control of virtual power plants, consideration of electricity and heat load demand response and low-carbon objectives can promote multienergy synergistic optimisation, ensuring a symmetrical power balance between system electricity, heat and gas, improving the stability and flexibility of system operation, and facilitating energy flow and interaction between system sources, storage and load.

(3) By introducing weighting coefficients for the sensitivity analysis of the system to form a comparison of optimal allocation options under different scenarios, the results show that different optimisation preference settings can significantly affect the system allocation results. The reasonable dispatch coefficients for the economic and environmental aspects of the VPP studied in the paper range from (r_1=0.7, r_2=0.3) ~ (r_1=0.4, r_2=0.6). In the future, by considering the degree of concern for different aspects in the optimisation process, suitable weighting coefficients can be selected to achieve flexible dispatch control of economic and environmental indicators.

References

[1] LAI S X, LU J P, LUO X Y, et al, "Carbon emission evaluation model and carbon reduction strategies for newly urbanized areas, " *Sustainable Production and Consumption*, vol.31, pp. 13-25, 2022.

[2] Zhang C , Xu Y , Dong Z Y . "Robustly Coordinated Operation of A Multi-Energy Micro-Grid in Grid-Connected and Islanded Modes under Uncertainties, " *IEEE Transactions on Sustainable Energy*, pp.1-1, 2019.

[3] Light Zaglago. Frank-K. Dzokoto, and Lynda Ankrah, "Challenges to Smart Grid Technology," Lecture Notes in Engineering and Computer Science: Proceedings of The World Congress on Engineering 2021, 7-9 July, 2021, London, U.K., pp175-180

[4] Miaomiao Wang, Qingwen Luo, Lulu Kuang, and Xiaoxi Zhu, "Optimized Rolling Grey Model for Electricity Consumption and Power Generation Prediction of China," *IAENG International Journal of Applied Mathematics*, vol. 49, no.4, pp.577-587, 2019.

[5] Rahimiyan M , Baringo L , "Strategic Bidding for a Virtual Power Plant in the Day-Ahead and Real-Time Markets: A Price-Taker Robust Optimization Approach," *IEEE Transactions on Power Systems*, vol.31, no.4, pp. 2676-2687, 2016.

[6] R. Liu, Y. Liu and Z. Jing, "Impact of Industrial Virtual Power Plant on Renewable Energy Integration," *2020 IEEE/IAS Industrial and Commercial Power System Asia (I&CPS Asia)*, pp. 1198-1202, 2020.

[7] João Soares, Mohammad Ali Fotouhi Ghazvini, Zita Vale, P.B. de Moura Oliveira, "A multi-objective model for the day-ahead energy resource scheduling of a smart grid with high penetration of sensitive loads," *Applied Energy*, vol 162, pp 1074-1088, 2016.

[8] Y. Wang, X. Ai, Z. Tan, L. Yan and S. Liu, "Interactive Dispatch Modes and Bidding Strategy of Multiple Virtual Power Plants Based on Demand Response and Game Theory," *IEEE Transactions on Smart Grid*, vol. 7, no. 1, pp. 510-519, 2016.

[9] X. Zhang, M. Shahidehpour, A. Alabdulwahab and A. Abusorrah, "Hourly Electricity Demand Response in the Stochastic Day-Ahead Scheduling of Coordinated Electricity and Natural Gas Networks," *IEEE Transactions on Power Systems*, vol. 31, no. 1, pp. 592-601, 2016.

[10] W J Niu, Y Li, B B Wang, "Virtual power plant modelling for demand response considering uncertainty," *Proceedings of the CSEE*, vol. 34, no. 22, pp. 3630-3637, 2014.

[11] T. F. Ma, J. Y. Wu, L. L. Hao, Y. J. Li, H. G. Yan, D. Z. Li and S. S. Chen, "Analysis of energy flow modeling and optimal operation of micro-energy networks based on energy hubs". *Power System Technology*, vol. 42, no. 01, pp. 179-186, 2018.

[12] Y. Y. Liu, C. W. Jiang, S. M. Tan, J. Z. Hu and Q. S. Li, "Optimal scheduling strategy for virtual power plants considering risk-adjusted capital return threshold constraint," *Proceedings of the CSEE*, vol. 36, no. 17, pp. 4617-4627, 2016.

[13] T. S. Li, J. L. Liu and M. Y. Wu, "Optimal scheduling of virtual power plants accounting for environmental costs," *Heilongjiang Electric Power*, vol.27, no.1, pp.5-12, 2015.

[14] Y Zhang, Q Xu and L Yang, "A study on the cooperation space between virtual power plants and conventional units considering carbon trading," *Energy Engineering*, vol. 5, pp. 1-7, 2016,

[15] G. Q. Sun, Y. Z. Zhou, Z. N. Wei, et al, "Robust optimization bidding model for virtual power plants under carbon emission constraints," *Proceedings of the CSEE*, vol. 37, no.11, pp. 3118-3128, 2017.

[16] Albadi M H , El-Saa Da Ny E F , "A summary of demand response in electricity markets," *Electric Power Systems Research*, vol. 78, no. 11, pp. 1989-1996, 2008.

[17] Gorostiza, Francisco Sanchez ; Gonzalez-Longatt, Francisco, "Optimised TSO–DSO interaction in unbalanced networks through frequency-responsive EV clusters in virtual power plants," *IET Generation Transmission & Distribution*, vol. 14, no. 21, pp. 4908-4917, 2020.

[18] D Kaczorowska, Rezmer J , Jasinski M , et al, "A Case Study on Battery Energy Storage System in a Virtual Power Plant: Defining Charging and Discharging Characteristics". *Energies*, vol.13, no.24, pp. 121-129, 2020.

[19] R. Gao, H. X. Guo, R. H. Zhang, T. Mao, Q. Y. Xu, B. R. Zhou and P. Yang. "A Two-Stage Dispatch Mechanism for Virtual Power Plant Utilizing the CVaR Theory in the Electricity Spot Market," *Energies*, vol. 12, no.17, pp. 1020-1029, 2019.

[20] C Y Ma, C F Dong, et al, "Short-term trading and optimal operating strategies for commercial virtual power plants accounting for stochastic factors," *Power System Technology*, vol. 40, no. 05, pp. 1543-1549, 2016.

[21] Fan S , Liu J , Wu Q , et al. Optimal Coordination of Virtual Power Plant with Photovoltaics and Electric Vehicles: A Temporally Coupled Distributed Online Algorithm[J]. Applied Energy, 2020, 277..

[22] Chen X Y, Kang C Q, O'Malley M , et al. "Increasing the Flexibility of Combined Heat and Power for Wind Power Integration in China: Modeling and Implications," *IEEE Transactions on Power Systems*, vol.30, no.4, pp. 1848-1857, 2015.

[23] Alhamed K, Dincer I, Lund H, et al. "Exergoeconomic analysis and optimization of a solar energy-based integrated system with oxy-combustion for combined power cycle and carbon capturing," *Energy*, vol.250, pp.123814, 2022.

[24] Z L Wei, S Yu, et al, "Concept and development of the micro-energy network," *Automation Of Electric Power Systems*, vol.37, no.13, pp. 1-9, 2013.